Pharmacological Research 187 (2023) 106562

Contents lists available at ScienceDirect

Pharmacological Research

journal homepage: www.elsevier.com/locate/yphrs

Liver lipopolysaccharide binding protein prevents hepatic inflammation in physiological and pathological non-obesogenic conditions☆

Edward Milbank [a,b,1], Ramon Díaz-Trelles [c,1], Nathalia Dragano [a,b], Jèssica Latorre [b,d], Rajesh Mukthavaram [c], Jordi Mayneris-Perxachs [b,d], Francisco Ortega [b,d], Massimo Federici [e], Remy Burcelin [f], Priya P. Karmali [c], Kiyoshi Tachikawa [c], Pad Chivukula [c], Miguel López [a,b], José Manuel Fernández-Real [b,d,g,*], José María Moreno-Navarrete [b,d,g,**]

[a] NeurObesity Group, Department of Physiology, CIMUS, University of Santiago de Compostela-Instituto de Investigación Sanitaria, Santiago de Compostela 15782, Spain
[b] CIBER Fisiopatología de la Obesidad y Nutrición (CIBERobn), and Instituto de Salud Carlos III (ISCIII), Madrid, Spain
[c] Arcturus Therapeutics, San Diego, CA 92121, USA
[d] Department of Diabetes, Endocrinology and Nutrition, Institut d'Investigació Biomèdica de Girona (IdIBGi), Girona, Spain
[e] Department of Systems Medicine, University of Rome Tor Vergata, Via Montpellier, Rome, Italy
[f] Institut des Maladies Métaboliques et Cardiovasculaires, INSERM U1048, Université Paul Sabatier, Toulouse, France
[g] Department of Medicine, University of Girona, Girona, Spain

ARTICLE INFO

Keywords:
LPS-binding protein
Lipid nanoparticles
SiRNAs
Liver inflammation
NASH

ABSTRACT

Lipopolysaccharide binding protein (LBP) knockout mice models are protected against the deleterious effects of major acute inflammation but its possible physiological role has been less well studied. We aimed to evaluate the impact of liver LBP downregulation (using nanoparticles containing siRNA- Lbp) on liver steatosis, inflammation and fibrosis during a standard chow diet (STD), and in pathological non-obesogenic conditions, under a methionine and choline deficient diet (MCD, 5 weeks). Under STD, liver *Lbp* gene knockdown led to a significant increase in gene expression markers of liver inflammation (*Itgax, Tlr4, Ccr2, Ccl2* and *Tnf*), liver injury (*Krt18* and *Crp*), fibrosis (*Col4a1, Col1a2* and *Tgfb1*), endoplasmic reticulum (ER) stress (*Atf6, Hspa5* and *Eif2ak3*) and protein carbonyl levels. As expected, the MCD increased hepatocyte vacuolation, liver inflammation and fibrosis markers, also increasing liver Lbp mRNA. In this model, liver *Lbp* gene knockdown resulted in a pronounced worsening of the markers of liver inflammation (also including CD68 and MPO activity), fibrosis, ER stress and protein carbonyl levels, all indicative of non-alcoholic steatohepatitis (NASH) progression. At cellular level, *Lbp* gene knockdown also increased expression of the proinflammatory mediators (*Il6, Ccl2*), and markers of fibrosis (*Col1a1, Tgfb1*) and protein carbonyl levels. In agreement with these findings, liver *LBP* mRNA in humans positively correlated with markers of liver damage (circulating hsCRP, ALT activity, liver *CRP* and *KRT18* gene expression), and with a network of genes involved in liver inflammation, innate and adaptive immune system, endoplasmic reticulum stress and neutrophil degranulation (all with q-value<0.05). In conclusion, current findings suggest that a significant downregulation in liver LBP levels promotes liver oxidative stress and inflammation, aggravating NASH progression, in physiological and pathological non-obesogenic conditions.

1. Introduction

Lipopolysaccharide-binding protein (LBP) is a 65-kDa acute-phase protein present in blood at high concentrations, known to be derived from the liver [1]. The binding to bacterial lipopolysaccharide (LPS), as its name indicates, is one of its best known functions but LBP is also a

☆ Abbreviated Title: Liver LBP prevents NASH progression

* Correspondence to: Department of Diabetes, Endocrinology and Nutrition (UDEN) Biomedical Research Institute of Girona "Dr Josep Trueta" Hospital of Girona "Dr Josep Trueta" Carretera de França s/n, 17007, Girona, Spain.

** Correspondence to: Section of Nutrition, Eumetabolism and Health Biomedical Research Institute of Girona "Dr Josep Trueta" C/ Dr.Castany s/n, 17190 Salt, Spain.

E-mail addresses: jmfreal@idibgi.org (J.M. Fernández-Real), jmoreno@idibgi.org (J.M. Moreno-Navarrete).

[1] These authors shared co-first authorship

https://doi.org/10.1016/j.phrs.2022.106562
Received 3 October 2022; Received in revised form 9 November 2022; Accepted 16 November 2022
Available online 21 November 2022

member of a family of lipid-binding proteins that also contains cholesteryl ester transfer protein and phospholipid transfer protein [2,3]. At high LBP concentrations, the LPS-induced inflammatory response is progressively attenuated either by transferring LPS into lipoproteins (such as HDL), by interfering on LPS interactions with the extracellular domains of membrane CD14 and TLR4-MD-2 receptor complex or by the formation of large extracellular LBP-LPS complexes that have a reduced ability to stimulate cells [1–8].

The role of liver LBP in acute and major inflammation has been well studied. LBP KO mice are protected from acetoaminophen-induced [9] and alcohol-induced liver injury [10]. LBP KO mice are also protected against the acute inflammation induced by biliary obstruction [11], hemorrhagic shock and granulocyte colony stimulating factor [12,13]. The inhibitory peptide LBPK95A also exerted beneficial effects in these situations [9–13]. LBP KO mice also had a significant reduction in liver steatosis, inflammation and fibrosis after a high-fat, high-sucrose and high-cholesterol diet [14]. Otherwise, specific liver *Lbp* gene knockdown prevented the progression of fatty liver in obesogenic conditions, resulting in a significant reduction in high-fat and high-sucrose diet-induced lipogenesis and liver lipid accumulation, without any effects on markers of liver damage and inflammation [15].

The role of LBP in physiology under a standard diet (STD) has been less studied. Here we aimed to investigate the effects of LBP downregulation on liver steatosis, inflammation and fibrosis under STD. Next, we also aimed to investigate the effects of LBP downregulation in pathological non-obesogenic conditions (methionine and choline deficient diet). The results of these experiments were in line with those of a liver transcriptomics study performed in humans.

2. Methods

2.1. Preparation of LUNAR®-Lbp UNA-siRNA

Using LUNAR® technology, a proprietary lipid enabled nucleic acid delivery platform, Arcturus Therapeutics (San Diego, CA) produced LUNAR® particles encapsulating *Lbp*-UNA siRNA as described previously [15,16]. LUNAR® is composed of four lipid components: Proprietary Arcturus Therapeutics's lipid (ATX), cholesterol, a phospholipid 1,2-distearoyl-sn-glycero-3-phosphocholine (DSPC), and a pegylated lipid. The ATX lipid contains an ionizable amino head group and a biodegradable lipid backbone. The ionizable amino head group provides the lipid with a pK_a of < 7. At acidic pH, the amino group is protonated and interacts with the negatively charged RNA, thus forming nanoparticles and encapsulating the RNA. However, at physiological pH, which is above the pK_a of the amino head group, LUNAR® nanoparticles stand neutral charge, attenuating the toxicity commonly observed with positively charged cationic transfection vectors. The pH sensitivity of the amino head group also enables protonation of the lipid once inside the endosomes, thereby promoting their interaction with the oppositely charged anionic endosomal lipids, causing destabilization of the endosomal membrane and release of RNA payload into the cytosol. In addition, ester groups, incorporated into the lipidic backbone of ATX lipids, produce ester bonds that have good chemical stability at physiological pH but can be easily cleaved by esterases inside tissue and intracellular compartments once the load has been delivered. Finally, the remnant hydrophilic cleavage products can be quickly metabolized. Briefly, UNA siRNA was dissolved in 2 mM citrate buffer, pH 3.5. Lipids at the desired molar ratio were dissolved in ethanol. The molar ratio of the constituent lipids is 58 % ATX (proprietary ionizable amino lipid), 7 % DSPC (1, 2-distearoyl-sn-glycero-3-phosphocholine) (Avanti Polar Lipids, Alabaster, AL, USA), 33.5 % cholesterol (Avanti Polar Lipids, Alabaster, AL, USA), and 1.5 % DMG-PEG (1,2-Dimyristoyl-sn-glycerol, methoxypolyethylene glycol, PEG chain Molecular weight: 2000) (NOF America Corporation, White Plains, NY). Lipid solution was then combined with UNA siRNA solution using a Nanoassemblr® microfluidic device (Precision NanoSystems Inc., Vancouver, Canada) at a flow rate ratio of 1:3 ethanol:aqueous phases. The mixed material was then diluted with 3X volume of 10 mM Tris buffer, pH 7.4 containing 9% sucrose, reducing the ethanol content to 6.25 %. The diluted formulation was then concentrated by tangential flow filtration using hollow fiber membranes (mPES Kros membranes, 100 Kd MWCO, Spectrum Laboratories, Inc., Rancho Dominguez, California), followed by diafiltration against 10 volumes of 10 mM Tris buffer, pH 7.4 containing 9% sucrose. Post diafiltration, formulations were then concentrated to desired UNA-siRNA concentration followed by filling into vials and freezing. Particle size was determined by dynamic light scattering (ZEN3600, Malvern Instruments). Encapsulation efficiency was calculated by determining unencapsulated UNA-siRNA content by measuring the fluorescence upon the addition of RiboGreen (Molecular Probes) to the particles (Fi) and comparing this value to the total RNA content that is obtained upon lysis of the particles by 1 % Triton X-100 (Ft), where % encapsulation $= (Ft - Fi)/Ft \times 100$.

2.2. Mice experiments

Eight-week-old male C57BL/6J mice ($N = 35$) were kept under 12 h light/dark cycle and had ad libitum access to standard diet or methionine and choline deficient (MCD) diet (A02082002BR, Research Diets) for 6 weeks. In the study, mice received weekly intravenous injections of LNP-UNA-C (siRNA-control or non-targeting siRNA) or LNP-UNA-LBP (siRNA-Lbp) (3 mg/kg) for 6 weeks (as shown in Supplementary Fig. 1). The selection of concentrations, doses, route and frequency of lipid nanoparticles (LNP) administration was based in previous experiments [15]. Food intake and body weight were weekly monitored. At week 6, after overnight fasting, mice were sacrificed by suffocation under sedation. Then, blood serum and liver were collected, immediately frozen in liquid-nitrogen, and stored at − 80 °C until processing for RNA, protein or histological analysis. A piece of liver was also fixed with 4% formalin for 24 h and then stored in 70 % ethanol at 4 °C for histological analysis. In all mice experiments, the research was conducted in accordance with the European Guidelines for the Care and Use of Laboratory Animals (directive 2010/63/EU) and animal protocols were approved by the Committee at the University of Santiago de Compostela.

2.3. In vitro experiments with lentiviral shRNA-Lbp particles

Four different short-hairpin-Lbp (clone set against mouse Lbp, NM_008489.2) primer sequences and random negative control (NC) sequence that did not have targets for any gene were synthesized by Tebu-bio (Tebu-bio, Spain, SL). Lentivirus-targeted Lbp was obtained by cotransfection of shRNA plasmids against Lbp and a combination of packaging and envelope plasmid from Addgene (pCMV-VSV-G and pCMV-dR8.2 dvpr) into HEK293T using LipoD293 transfection reagent following manufacturers' instructions. Mouse hepatoma Hepa1–6 cell line was purchased from American Type Culture Collection (*ATCC, Virginia, EUA*) and cultured in Dulbecco's Modified Eagle's Medium (DMEM) supplemented with 4500 mg/L glucose, 10 % fetal bovine serum (Gibco), 100 units/ml penicillin and streptomycin, 1 % glutamine and 1 % sodium pyruvate, at 37 °C and 5 % CO2 atmosphere. Gene silencing was achieved using *Lbp*-targeted and control shRNA lentiviral particles. Stable clones expressing the shRNA were selected by puromycin dihydrochloride. Four biological replicates were collected from 2 independent experiments.

2.4. Human study

Participants ($n = 82$) were recruited at Hospital Universitari Dr Josep Trueta of Girona and Policlinico Tor Vergata University of Rome. Information about anthropometric and clinical parameters, inclusion and exclusion criteria, and the transcriptomics study was detailed elsewhere [17]. Inclusion criteria were that all subjects were of Caucasian origin, reported a stable body weight 3 months preceding the study, were not

given a liquid diet before surgery, were free of any infections (including use of antibiotics 1 month before surgery) and had no systemic disease. In brief, hybridization of the Agilent Whole Human Genome Oligo Microarrays, 4 × 44 K was done according to the Agilent 60-mer oligo microarray processing protocol using the Agilent Gene Expression Hybridization Kit. After two washes with Agilent Gene Expression Wash Buffer and one with acetonitrile, the fluorescence signals of the hybridized Agilent microarrays were detected using Agilent's Microarray Scanner System. The image files were read using Agilent Feature Extraction Software to determine feature intensities (i.e. to produce the raw data). All subjects gave written informed consent in accordance with the Declaration of Helsinki, after the purpose of the study was explained to them. The protocol was approved by the ethical committee of the Hospital Universitari Dr Josep Trueta (Comitè d'Ètica d'Investigació Clínica, approval number 2009 046) and Policlinico Tor Vergata University of Rome (Comitato Etico Indipendente, approval number 28–05–2009) [17].

2.5. Gene expression analysis

RNA purification (isolation) was performed using the RNeasy Lipid Tissue Mini Kit (QIAgen, Izasa SA, Barcelona, Spain) and the integrity was checked by the Agilent Bioanalyzer (Agilent Technologies, Palo Alto, CA). Gene expression was assessed by real-time PCR using a LightCycler® 480 Real-Time PCR System (Roche Diagnostics SL, Barcelona, Spain), using TaqMan® technology suitable for relative genetic expression quantification. The commercially available and pre-validated TaqMan® primer/probe sets used were as follows: Endogenous control *18S*, and target gene mouse lipopolysaccharide binding protein (*Lbp,* Mm00493139_m1); fatty acid binding protein 4, adipocyte (*Fabp4*, Mm00445878_m1); collagen, type IV, alpha 1 (*Col4a1*, Mm01210125_m1); collagen, type I, alpha 2 (*Col1a2*, Mm00483888_m1); collagen, type I, alpha 1 (*Col1a1*, Mm00801666_g1); transforming growth factor, beta 1 (*Tgfb1*, Mm01178820_m1); interleukin 6, (*Il6*, Mm00446190_m1); tumor necrosis factor (*Tnf*, Mm00443258_m1); integrin alpha X (*Itgax*, Mm00498701_m1); chemokine (C-C motif) ligand 2 (*Ccl2*, Mm00441242_m1); interleukin 10 (*Il10*, Mm01288386_m1); lactotransferrin (*Ltf*, Mm00434787_m1); toll-like receptor 4 (*Tlr4*, Mm00445273_m1); chemokine (C-C motif) receptor 2 (*Ccr2*, Mm99999051_gH); keratin 18 (*Krt18*, Mm01601704_g1); C-reactive protein, pentraxin-related (*Crp*, Mm00432680_g1); lymphocyte antigen 96 (*Ly96* or *MD2*, Mm01227593_m1); glutathione S-transferase, alpha 3 (*Gsta3*, Mm00494798_m1); glutathione peroxidase 4 (*Gpx4*, Mm00515041_m1); superoxide dismutase 2, mitochondrial (*Sod2*, Mm01313000_m1); activating transcription factor 6 (*Atf6*, Mm01295316_m1); heat shock protein 5 (*Hspa5*, Mm00517691_m1), eukaryotic translation initiation factor 2 alpha kinase 3 (*Eif2ak3*, Mm00438700_m1), DNA-damage inducible transcript 3 (*Ddit3*, Mm01135937_g1), eukaryotic translation initiation factor 2, subunit 1 alpha (*Eif2s1*, Mm00782766_s1).

2.6. Histological procedures

Frozen liver samples were cut in 8 μm sections with a cryostat and stained in filtered Oil Red O for 10 min. After being washed in distilled water, sections were counterstained with Mayer's hematoxylin for 3 min and mounted in aqueous mounting (glycerin jelly). Liver samples were fixed in 4 % formaldehyde for 24 h and then dehydrated and embedded in paraffin. For Sirius Red staining, samples fixated in paraffin were dewaxed, hydrated, and stained in PicroSirius staining red for one hour. Then, samples were washed with distilled water, dehydrated in three changes of 100 % ethanol, and cleared in xylene and mounted in a resinous medium. For CD68 immunohistochemistry staining, samples fixated in paraffin were dewaxed, hydrated, pre-treated in PTLink TE buffer pH 9, and blocked with 3 % peroxidase for 10 min. Then, sections were incubated with the primary antibody (ab125212, Abcam) at a concentration of 1:500 overnight and at 4 °C, followed by an incubation with the secondary antibody (EnVision, DAKO) for 30 min at room temperature. After that, DAB developer was used for 1 min and sections were counterstained with Mayer's hematoxylin for 10 min, dehydrated and mounted. In all the histological staining, up to 4 representative microphotographs of each animal at 20× or 40× were taken with a BX51 microscope equipped with a DP70 digital camera (Olympus). Lipids in Oil Red O- stained sections, collagen depositions in Sirius Red-stained sections and inflammatory infiltrates in CD68-stained sections were quantified using FRIDA software (Framework for Image Dataset Analysis, the Johns Hopkins University).

2.7. Liver myeloperoxidase (MPO) activity

Since MPO is abundantly expressed in neutrophils, measurement of its activity in liver is considered as a useful marker of neutrophil infiltration. Liver (~30 mg) was homogenized in 4 volumes of MPO Assay Buffer, centrifuged for 10 min at 13,000 *g* to remove insoluble material and collecting supernatant for assay. MPO activity was measured using Myeloperoxidase (MPO) Activity Colorimetric Assay Kit (Cat nº: K744–100, Biovision Inc., CA, USA) following the manufacture's protocol.

2.8. Protein carbonyl measurement

Liver protein carbonyl was measured by Protein Carbonyl Content Assay Kit (Cat nº: MAK094, Merck Life Science S.L.U., Madrid, Spain), being liver (~20 mg) samples processed and assayed strictly following the manufacture's protocol.

2.9. Liver LPS measurement

Liver LPS was measured using Mouse Lipopolysaccharides (LPS) ELISA Kit (Cat nº: CBS-E13066m, CUSABIO TECHNOLOGY LLC, Wuhan, China). Liver (~50 mg) was homogenized in 0.5 ml of sterile PBS and stored overnight at − 20ºC. After two freeze-thaw cycles were performed to break the cell membranes, the homogenates were centrifuged for 5 min at 5000× g, 2–8 ºC. The supernatant was removed and assayed immediately following the manufacture's protocol. To validate the assay accuracy and especificity a positive control of *Escherichia coli* O26:B6-derived LPS (L2654, Merck Life Science S.L.U., Madrid, Spain) was included.

2.10. Serum/plasma measurements

In mice, plasma LBP (HK205–02, LBP mouse ELISA kit, Hycult Biotech *Inc.,* PA, USA), insulin (90080), leptin (90030) and adiponectin (80569, Crystal Chem, Zaandam, Netherlands), glucose (Accutrend; Roche Diagnostics, Mannheim, Germany), and alanine transaminase (ALT) activity (Alfa Wasserman/Vet Axcel Reagent SA1046) were measured using commercial kits according to manufacturer' instructions. Serum sCD14 levels were analyzed by Quantikine ELISA Mouse CD14 Immunoassay (MC140, R&D Systems, Inc., MN, USA). Serum LPS levels were analyzed by Limulus amebocyte lysate (LAL) chromogenic Endpoint Assay (HIT302, HyCult Biotech Inc., PA, USA) following manufacturer's instructions. Prior to serum LPS analysis, serum endotoxin inhibiting compounds were neutralized by heating the sample at 75 °C for 5 min.

In human study, C-reactive protein (ultrasensitive assay; 110 Beckman, Fullerton, CA, United States) was determined by a routine laboratory test.

2.11. Statistical analysis

Statistical analyses were performed using the SPSS 12.0 software. In

mice and in in vitro experiments, all results are expressed as means ± SEM, and differences were tested for statistical significance using Student's unpaired *t*-test in mice and non-parametric tests (Mann–Whitney U test) in in vitro experiments. In human study, the relation between variables was analyzed by simple correlation (using Spearman's correlation coefficient). Levels of statistical significance were set at $p < 0.05$.

Pathway analysis. Differentially expressed genes associated with liver *LBP* mRNA were annotated to a pathway-level via over-representation analysis using the IMPaLA [18]. The list of genes of interest and a background list of all measured genes was compared and upload. Then, a hypergeometric test was used to assess the significance of each pathway in terms of its overlap with those lists and a Storey procedure (q-values) was applied for multiple testing correction.

3. Results

3.1. Liver Lbp knockdown results in liver oxidative stress, inflammation and fibrosis under STD

In mice fed a standard chow diet (STD), weekly LNP-UNA-LBP (siRNA-Lbp) administration downregulated liver *Lbp* gene expression and decreased serum LBP levels (Fig. 1A), but did not impact on adipose tissue *Lbp* gene expression [19]. No significant changes were observed in body weight, fasting blood glucose, insulin, $HOMA_{IR}$, leptin, adiponectin, the liver injury marker ALT, serum sCD14 and circulating LPS levels (Supplementary Fig. 2A-I). *Lbp* gene knockdown also induced no changes on H&E and Oil red O staining or the expression of the *Fabp4* gene (Supplementary Fig. 2J-K).

Liver *Lbp* gene knockdown resulted in a significant increase in gene expression markers of liver inflammation (*Itgax, Tlr4, Ccr2, Ccl2* and *Tnf*) and injury (*Krt18* and *Crp*), without significant differences in CD68 staining, MPO activity or liver LPS levels (Fig. 1B-E). Gene expression markers of fibrosis (*Col4a1, Col1a2* and *Tgfb1*) were also significantly increased but without significant differences in the Sirius Red (Fig. 1F-G). Increased ER stress markers (*Atf6, Hspa5* and *Eif2ak3*), antioxidant response genes (*Gsta3, Gpx4* and *Sod2*) and protein carbonyl levels, reflecting increased intracellular reactive oxygen species (Fig. 1H-J), were also observed.

3.2. Liver Lbp knockdown aggravates liver inflammation in mice fed a methionine and choline deficient diet (MCD)

In mice fed a methionine and choline deficient diet (MCD), liver *Lbp* gene expression, but not serum LBP, were significantly increased compared to STD (Supplementary Table 1). MCD led to a significant reduction in body weight, fasting blood glucose, insulin, and leptin levels, increasing adiponectin, ALT and serum sCD14 levels, but decreasing serum LPS levels (Supplementary Table 1). As expected, the

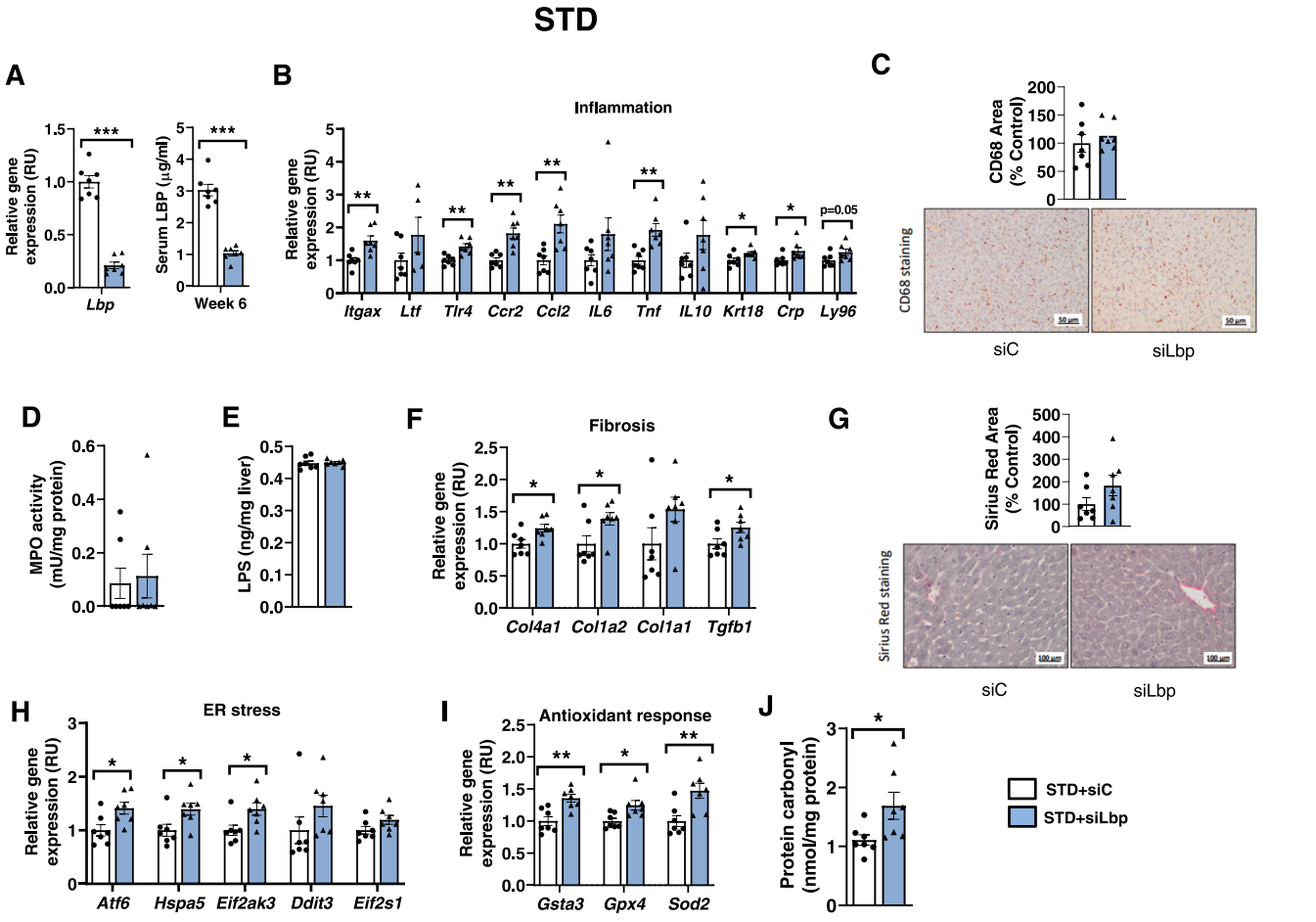

Fig. 1. Impact of liver *Lbp* gene knockdown on liver inflammation, fibrosis, ER stress and oxidative stress in STD-fed mice. A-J) Effects of weekly LNP-*Lbp* UNA-siRNA administration in STD-fed mice on liver *Lbp* mRNA and serum LBP (A), liver inflammation (B-D) [including inflammation (*Itgax, Ltf, Tlr4, Ccr2, Ccl2, Il6, Tnf, Il10, Krt18* and *Crp*)-related gene expression (B), representative CD68 staining histological liver slides (20X) and CD68 positive cells area (C) and MPO activity (D)], liver LPS levels (E), liver fibrosis (F-G) [including fibrosis (*Col4a1, Col1a2, Col1a1* and *Tgfb1*)-related gene expression (F) and representative Sirius Red staining histological liver slides (20X) and Sirius Red area (G)], expression of ER stress- and antioxidant response-related genes (H-I) and the marker of oxidative stress protein carbonyl (J). *$p < 0.05$, **$p < 0.01$ and ***$p < 0.001$ compared to vehicle (siC). STD: Standard diet; siLbp: Weekly LNP-*Lbp* UNA-siRNA (3 mg/kg) administration. Data were tested for statistical significance using Student's unpaired *t*-test.

MCD increased hepatocyte vacuolation in H&E staining and Oil red O area in parallel to increased fatty acid uptake-related gene *Fabp4* mRNA (Supplementary Table 1). MCD-fed mice also displayed increased liver inflammation markers (*Itgax, Ltf, Tlr4, Ccr2, Ccl2, Tnf, Il10, Krt18* and *Ly96* mRNA and CD68 protein staining; Supplementary Table 2), decreased liver LPS levels (Supplementary Table 2), and increased markers of fibrosis (*Col4a1, Col1a2, Col1a1* and *Tgfb1* mRNA, in parallel to Sirius Red area; Supplementary Table 2), ER stress (*Atf6*, *Hspa5, Eif2ak3, Ddit3* and *Eif2s1*) and oxidative stress (*Gpx4* mRNA, protein carbonyl) (Supplementary Table 2).

Similar to STD, liver *Lbp* gene knockdown in MCD-fed mice (Fig. 2A) did not impact on metabolic parameters (body weight, fasting blood glucose, insulin, $HOMA_{IR}$, leptin, adiponectin), the liver injury marker ALT, serum sCD14, circulating LPS levels, *Fabp4* gene expression, but slightly increased liver lipid accumulation (as reflected increased Oil red O staining area) (Supplementary Fig. 3A-K). Strikingly, liver *Lbp* gene knockdown in MCD-fed mice resulted in a pronounced increase in markers of liver inflammation (*Itgax, Ccr2, Ccl2* and *Tnf* mRNA, CD68 and MPO activity), without significant differences again in liver LPS levels (Fig. 2B-E). Liver *Lbp* gene knockdown also increased the expression of fibrosis and ER stress markers and protein carbonyl levels, without significant differences in Sirius Red area and expression of antioxidant response-related genes in these mice (Fig. 2F-J).

3.3. *Lbp gene knockdown enhanced markers of inflammation and oxidative stress in the mouse Hepa1-6 cell line*

To gain insight in the potential mechanisms that underlie the impact of *Lbp* gene knockdown on liver inflammation, in vitro experiments in the murine Hepa1–6 cell line were performed. *Lbp* gene knockdown led to increased expression of the proinflammatory cytokine *Il6*, the chemokine *Ccl2*, and the markers of fibrosis (*Col1a1, Tgfb1*) and oxidative stress (protein carbonyl), but decreased gene expression of the LPS signaling receptor *Tlr4* and the acute phase protein *Crp* (Fig. 3A-D).

3.4. *Liver Lbp mRNA is associated with hepatic inflammation and increased in NASH*

In agreement with the findings in mice, liver *LBP* mRNA in humans also positively correlated with markers of liver damage, including circulating hsCRP, ALT activity, liver *CRP* and liver *Krt18* gene expression (Fig. 3E-H). Importantly, liver *LBP* was linked to different NASH-associated pathways like: (i) Immune system (q-value = 0.00000013); (ii) innate (q-value = 0.0013) and adaptative (q-value=0.032) immune system; and (iv) Neutrophil degranulation (q-value = 0.045) (Supplementary file 1; Fig. 3I) [20–23].

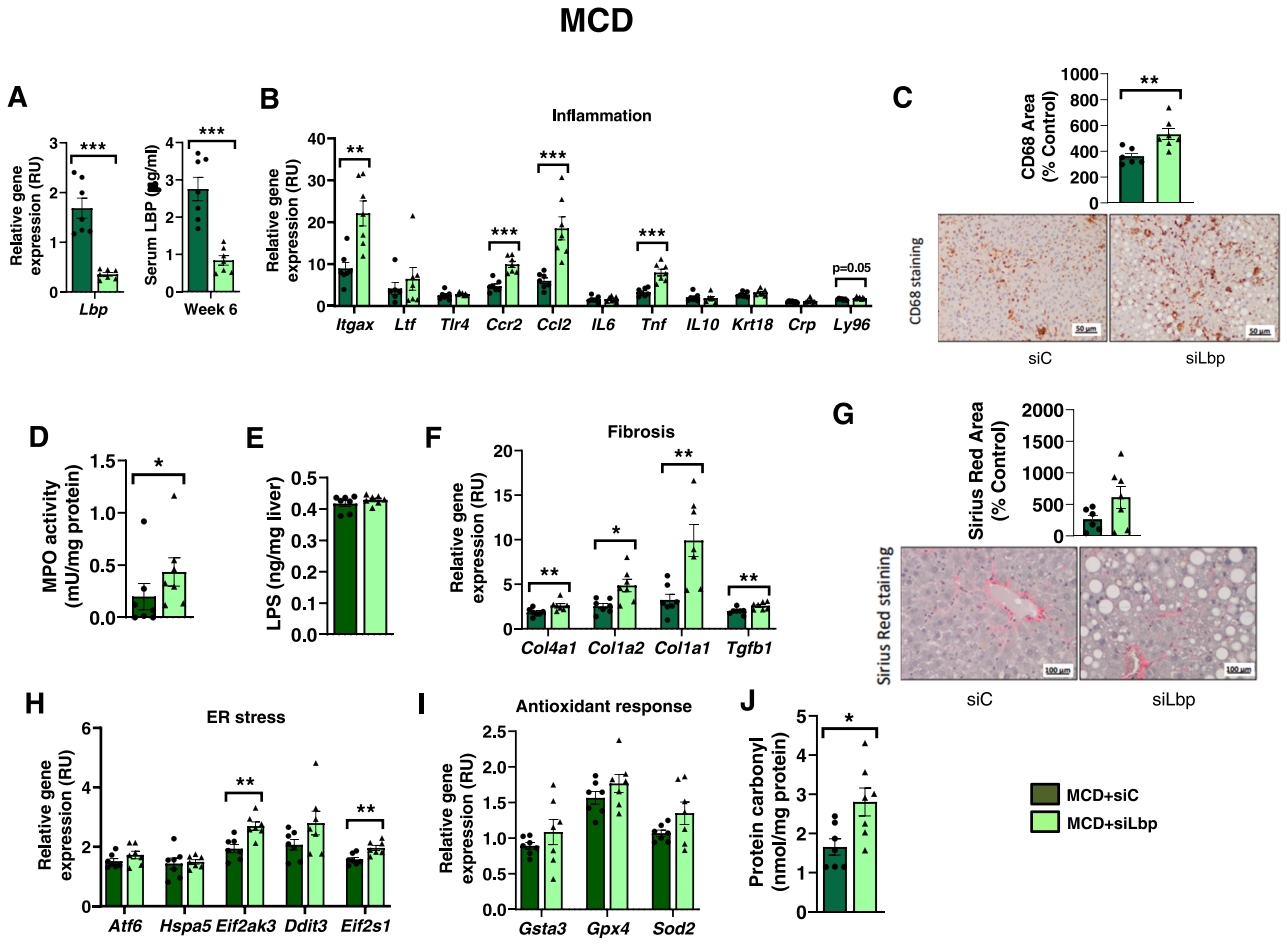

Fig. 2. Impact of liver *Lbp* gene knockdown on liver inflammation, fibrosis, ER stress and oxidative stress in MCD-fed mice. A-D) Effects of weekly LNP-*Lbp* UNA-siRNA administration in MCD-fed mice on liver *Lbp* mRNA and serum LBP (A), liver inflammation (B-D) [including inflammation (*Itgax, Ltf, Tlr4, Ccr2, Ccl2, Il6, Tnf, Il10, Krt18* and *Crp*)-related gene expression (B), representative CD68 staining histological liver slides (20X) and CD68 positive cells area (C) and MPO activity (D)], liver LPS levels (E), liver fibrosis (F-G) [including fibrosis (*Col4a1, Col1a2, Col1a1* and *Tgfb1*)-related gene expression (F) and representative Sirius Red staining histological liver slides (20X) and Sirius Red area (G)], expression of ER stress- and antioxidant response-related genes (H-I) and the marker of oxidative stress protein carbonyl (K). $^{*}p < 0.05$, $^{**}p < 0.01$ and $^{***}p < 0.001$ compared to vehicle (siC). MCD: Methionine and choline deficient diet; siLbp: Weekly LNP-*Lbp* UNA-siRNA (3 mg/kg) administration. Data were tested for statistical significance using Student's unpaired *t*-test.

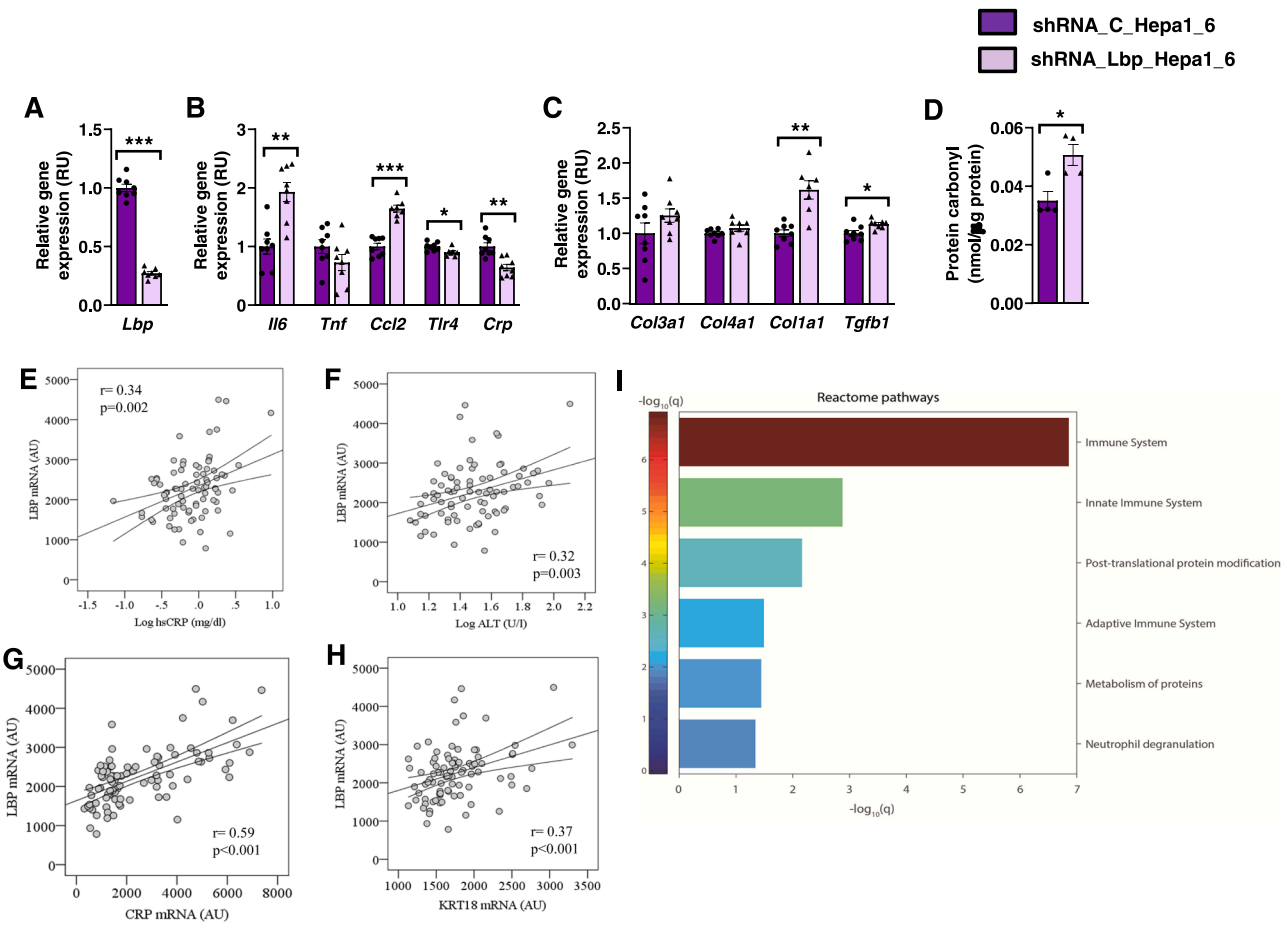

Fig. 3. Impact of *Lbp* gene knockdown on hepatocyte inflammation and oxidative stress and liver LBP levels in association to liver inflammation and NASH-associated pathways in humans. A-D) Effects of *Lbp* gene knockdown using lentiviral particles on expression of *Lbp*, inflammation (*Il6, Tnf, Ccl2, Tlr4, Crp*)- and fibrosis (*Col3a1, Col4a1, Col1a1, Tgfb1*)-related genes (A-C) and on protein carbonyl levels (D) in mouse Hepa1–6 cell line. *p < 0.05, **p < 0.01 and ***p < 0.001 compared to shRNA_C. Data were tested for statistical significance using non-parametric tests (Mann–Whitney U test). E-H) Bivariate correlations between liver *LBP* mRNA levels and serum hsCRP (E), serum ALT activity (F) and liver *CRP* (G) and *KRT18* (H) mRNA levels in humans. Bivariate correlations were analyzed by simple correlation (using Spearman's correlation coefficient). Levels of statistical significance were set at p < 0.05. I) This figure represents reactome pathways associated with liver *LBP* mRNA levels in human liver. These reactome pathways included a large number of genes, most of which were enriched in pathways that have been strongly associated to liver steatosis. A hypergeometric test was used to assess the significance of each pathway in terms of its overlap with those lists and a Storey procedure (q-values) was applied for multiple testing correction.

4. Discussion

Under physiological conditions, the current findings point to a protective role of liver Lbp in the prevention of liver inflammation, oxidative stress and fibrosis. Mice under STD treated with LNP-*Lbp* UNA-siRNA, showed increased liver inflammation in parallel to a reduction of LBP without changes in LPS levels, suggesting an enhanced LPS-induced inflammatory response. Supporting this idea, a decrease in LBP concentrations is associated with an enhanced inflammatory response to LPS [1–8]. Very recent studies have shown that intestine-derived HDL traverses the portal vein in the HDL3 subspecies to form a complex with LBP, preventing LPS-induced liver inflammation [24]. In agreement with these findings, in a rat sepsis model, increased LPS-induced liver ballooning degeneration and ROS production was observed in LBP$^{-/-}$ rat livers [25]. However, in vitro experiments point to a direct effect of *Lbp* gene knockdown in the induction of hepatocyte inflammation and oxidative stress in the absence of LPS stimulus.

Interestingly, the induction of the proinflammatory cytokine Il6 and the chemokine Ccl2, which has a key role in tissue monocyte recruitment, observed in *Lbp* gene knockdown hepatocytes suggests a possible mechanism to explain in part the onset of *Lbp* gene knockdown-associated liver inflammation.

In addition, the previously described protective effect of LBP on hepatic mitochondria [25] also suggest that the reduction in LBP levels might increase oxidative stress, and in consequence promotes hepatocyte inflammation [26]. In line with this, increased protein carbonyl levels, which reflect increased intracellular reactive oxygen species, were observed in liver (in vivo experiments) and hepatocytes (Hepa1–6 in vitro experiment) after knockdown of *Lbp* gene in normal conditions.

In the experimental NASH mouse model (under a MCD), liver *Lbp* gene knockdown has an additive effect on liver inflammation, in which the increased sensitivity to LPS adds to the pro-inflammatory effect of MCD-induced lipotoxicity. This proinflammatory effect of liver *Lbp* gene knockdown resulted in a significant increase in expression of fibrosis- and ER stress-related genes and also was associated to increased protein carbonyl levels, the oxidative stress marker associated to severe liver damage [27].

The proinflammatory response obtained from the reduction of liver and circulating LBP levels in MCD and physiological conditions are in sharp contrast to the previous observations in LBP KO experimental mice models [9–14]. These discrepancies suggest different responses in situations of post-natal reduction of LBP levels compared to the total absence of this protein from embryonic development and might be explained by compensatory mechanisms.

It is interesting to highlight that, in animal models of hepatic ischemia reperfusion injury and liver transplantation, both the translocation of LPS and liver LBP expression are known to be increased [28–30]. Further studies are necessary to investigate the local effects after the administration of LPS alone or in combination with other hepatoxins. However, it should be borne in mind that unintended variations in the preparation of the LPS solution or in handling of the animals might affect the reproducibility or the outcome of a specific experiment.

Although the MCD diet is an optimal dietary model to produce liver steatosis, inflammation and even fibrosis in few weeks, its physiological relevance is very limited, especially as mice loss body weight instead of developing overweight and do not develop insulin resistance both being hallmarks of the development of non-alcoholic fatty liver disease (NAFLD). In contrast and as expected, high-fat and high-sucrose (HFHS) diet (during 25 weeks) resulted in increased body weight, fat mass and insulin resistance in parallel to liver steatosis and inflammation [15]. While MCD diet increased liver Lbp expression but did not change circulating LBP levels (current data), HFHS diet increased adipose tissue and circulating LBP levels, without any effect on liver Lbp gene and protein expression [15,19]. These results indicated that long-term liver damage (produced by lipotoxicity and metabolic endotoxemia) did not impact on liver Lbp biosynthesis, and confirmed that Lbp has an acute phase protein expression pattern in liver [7–10]. Supporting a possible protective role of liver LBP induction in situations of acute liver damage, liver *Lbp* gene knockdown in HFHS-fed mice, which developed NAFLD-associated chronic low-level liver inflammation but not acute inflammation as observed in NASH, did not impact on liver inflammation or markers of liver damage [15].

Another difference between HFHS and MCD diets were their impact on circulating LPS levels. While HFHS diet resulted in increased serum LPS levels, and this increase was attenuated by liver *Lbp* gene knockdown [19], MCD diet led to decreased serum LPS levels compared to standard diet, and no significant effects of liver *Lbp* gene knockdown were observed in these situations. These data indicate that metabolic endotoxemia produced by high-fat diet-associated gut dysbiosis [31,32] does not occur in mice fed with MCD for 5 weeks, and support that the pro-inflammatory effect of MCD depends more on lipotoxicity than LPS, and that the pro-inflammatory effect of *Lbp* gene knockdown did not depend on LPS levels.

Current findings suggest that a significant downregulation in liver LBP levels promotes liver oxidative stress and inflammation, aggravating NASH progression. This study provides novel and relevant information for the design of new therapeutic approaches to ameliorate this important pathological condition. However, further studies evaluating the effect of liver LBP overexpression in MCD-fed mice are required to further demonstrate whether liver LBP has a protective and compensatory role in the modulation of liver inflammation in NASH.

CRediT authorship contribution statement

Ramon Díaz-Trelles, José Manuel Fernández-Real and José María Moreno-Navarrete participated in study design and analysis of data. **Edward Milbank, Ramon Díaz-Trelles, Nathalia Dragano, Jessica Latorre, Rajesh Mukthavaram, Jordi Mayneris-Perxachs, Francisco Ortega, Priya P. Karmali and José María Moreno-Navarrete** participated in acquisition of data. **Edward Milbank, Ramon Díaz-Trelles, Nathalia Dragano, Massimo Federici, Remy Burcelin, Kiyoshi Tachikawa, Pad Chivukula, Miguel López, José Manuel Fernández-Real and José María Moreno-Navarrete** participated in interpretation of data. **José María Moreno-Navarrete** wrote and edited the manuscript. **Edward Milbank, Ramon Díaz-Trelles, Nathalia Dragano, Kiyoshi Tachikawa, Miguel López and José Manuel Fernández-Real** revised the manuscript critically for important intellectual content. All authors participated in final approval of the version to be published.

Conflict of interest

Ramon Díaz-Trelles, Rajesh Mukthavaram, Priya P. Karmali, Kiyoshi Tachikawa and Pad Chivukula are employees of Arcturus Therapeutics. The authors declared no additional conflict of interest.

Data availability

Data will be made available on request.

Acknowledgments

We acknowledge the technical assistance of Oscar Rovira (IdIBGi) in human sample collection. This work was partially supported by research grants PI16/02173, PI19/01712 and PI21/01361 from the Instituto de Salud Carlos III from Spain, FEDER funds and was also supported by Fundació Marató de TV3 (201612–31). CIBEROBN Fisiopatología de la Obesidad y Nutrición is an initiative from the Instituto de Salud Carlos III from Spain.

Authors' contributions

RD-T, JMF-R and JMM-N participated in study design and analysis of data. EM, RD-T, ND, JL, RM, JM-P, FO, PPK and JMM-N participated in acquisition of data. EM, RD-T, ND, MF, RB, KT, PC, ML, JMF-R and JMM-N participated in interpretation of data. JMM-N wrote and edited the manuscript. EM, RD-T, ND, KT, ML and JMF-R revised the manuscript critically for important intellectual content. All authors participated in final approval of the version to be published.

Appendix A. Supporting information

Supplementary data associated with this article can be found in the online version at doi:10.1016/j.phrs.2022.106562.

References

[1] J. Zweigner, H.J. Gramm, O.C. Singer, K. Wegscheider, R.R. Schumann, High concentrations of lipopolysaccharide-binding protein in serum of patients with severe sepsis or septic shock inhibit the lipopolysaccharide response in human monocytes, Blood 98 (2001) 3800–3808.
[2] Y. Sun, L. Li, J. Wu, P. Yu, C. Li, J. Tang, et al., Bovine recombinant lipopolysaccharide binding protein (BRLBP) regulated apoptosis and inflammation response in lipopolysaccharide-challenged bovine mammary epithelial cells (BMEC), Mol. Immunol. 65 (2015) 205–214.
[3] T. Gutsmann, M. Müller, S.F. Carroll, R.C. MacKenzie, A. Wiese, U. Seydel, Dual role of lipopolysaccharide (LPS)-binding protein in neutralization of LPS and enhancement of LPS-induced activation of mononuclear cells, Infect. Immun. 69 (2001) 6942–6950.
[4] L. Hamann, C. Stamme, A.J. Ulmer, R.R. Schumann, Inhibition of LPS-induced activation of alveolar macrophages by high concentrations of LPS-binding protein, Biochem. Biophys. Res Commun. 295 (2002) 553–560.
[5] S. Knapp, S. Florquin, D.T. Golenbock, T. van der Poll, Pulmonary lipopolysaccharide (LPS)-binding protein inhibits the LPS-induced lung inflammation in vivo, J. Immunol. 176 (2006) 3189–3195.
[6] P.A. Thompson, P.S. Tobias, S. Viriyakosol, T.N. Kirkland, R.L. Kitchens, Lipopolysaccharide (LPS)-binding protein inhibits responses to cell-bound LPS, J. Biol. Chem. 278 (2003) 28367–28371.
[7] L. Hamann, C. Alexander, C. Stamme, U. Zähringer, R.R. Schumann, Acute-phase concentrations of lipopolysaccharide (LPS)-binding protein inhibit innate immune cell activation by different LPS chemotypes via different mechanisms, Infect. Immun. 73 (2005) 193–200.
[8] R.L. Kitchens, P.A. Thompson, Modulatory effects of sCD14 and LBP on LPS-host cell interactions, J. Endotoxin Res. 11 (2005) 225–229.
[9] G.L. Su, K.Q. Gong, M.H. Fan, W.M. Kelley, J. Hsieh, J.M. Sun, et al., Lipopolysaccharide-binding protein modulates acetaminophen-induced liver injury in mice, Hepatology 41 (2005) 187–195.
[10] T. Uesugi, M. Froh, G.E. Arteel, B.U. Bradford, M.D. Wheeler, E. Gäbele, et al., Role of lipopolysaccharide-binding protein in early alcohol-induced liver injury in mice, J. Immunol. 168 (2002) 2963–2969.
[11] R.M. Minter, X. Bi, G. Ben-Josef, T. Wang, B. Hu, S. Arbabi, et al., LPS-binding protein mediates LPS-induced liver injury and mortality in the setting of biliary obstruction, Am. J. Physiol. - Gastrointest. Liver Physiol. 296 (2009) 45–55.

[12] H. Fang, A. Liu, J. Sun, A. Kitz, O. Dirsch, U. Dahmen, Granulocyte colony stimulating factor induces lipopolysaccharide (LPS) sensitization via upregulation of LPS binding protein in rat, PLOS One 8 (2013), e56654.
[13] M. Lehnert, T. Uehara, B.U. Bradford, H. Lind, Z. Zhong, D.A. Brenner, et al., Lipopolysaccharide-binding protein modulates hepatic damage and the inflammatory response after hemorrhagic shock and resuscitation, Am. J. Physiol. - Gastrointest. Liver Physiol. 291 (2006) G456–G463.
[14] C.J. Jin, A.J. Engstler, D. Ziegenhardt, S.C. Bischoff, C. Trautwein, I. Bergheim, Loss of lipopolysaccharide-binding protein attenuates the development of diet-induced non-alcoholic fatty liver disease in mice, J. Gastroenterol. Hepatol. 32 (2017) 708–715.
[15] J. Latorre, R. Díaz-Trelles, F. Comas, A. Gavaldà-Navarro, E. Milbank, N. Dragano, et al., Downregulation of hepatic lipopolysaccharide binding protein improves lipogenesis-induced liver lipid accumulation, Mol. Ther. Nucleic Acids 29 (2022) 599–613.
[16] S. Ramaswamy, N. Tonnu, K. Tachikawa, P. Limphong, J.B. Vega, P.P. Karmali, et al., Systemic delivery of factor IX messenger RNA for protein replacement therapy, Proc. Natl. Acad. Sci. USA 114 (2017) E1941–E1950.
[17] L. Hoyles, J.M. Fernández-Real, M. Federici, M. Serino, J. Abbott, J. Charpentier, et al., Molecular phenomics and metagenomics of hepatic steatosis in non-diabetic obese women, Nat. Med. 24 (2018) 1070–1080.
[18] A. Kamburov, R. Cavill, T.M. Ebbels, R. Herwig, H.C. Keun, Integrated pathway-level analysis of transcriptomics and metabolomics data with IMPaLA, Bioinformatics 27 (2011) 2917–2918.
[19] F. Comas, R. Díaz-Trelles, A. Gavaldà-Navarro, E. Milbank, N. Dragano, S. Morón-Ros, et al., Downregulation of peripheral lipopolysaccharide binding protein impacts on perigonadal adipose tissue only in female mice, Biomed. Pharmacother. 151 (2022), 113156, https://doi.org/10.1016/j.biopha.2022.113156.
[20] S. Sookoian, C.J. Pirola, Review article: shared disease mechanisms between non-alcoholic fatty liver disease and metabolic syndrome – translating knowledge from systems biology to the bedside, Aliment Pharm. Ther. 49 (2019) 516–527.
[21] J. Hundertmark, O. Krenkel, F. Tacke, Adapted immune responses of myeloid-derived cells in fatty liver disease, Front. Immunol. 9 (2018) 2418.
[22] C. Lebeaupin, D. Vallée, Y. Hazari, C. Hetz, E. Chevet, B. Bailly-Maitre, Endoplasmic reticulum stress signalling and the pathogenesis of non-alcoholic fatty liver disease, J. Hepatol. 69 (2018) 927–947.
[23] A.S. Henkel, Unfolded protein response sensors in hepatic lipid metabolism and nonalcoholic fatty liver disease, Semin. Liver Dis. 38 (2018) 320–332.
[24] Y.-H. Han, E.J. Onufer, L.-H. Huang, R.W. Sprung, W.S. Davidson, R. S. Czepielewski, et al., Enterically derived high-density lipoprotein restrains liver injury through the portal vein, Science 23 (2021) 6553.
[25] Z. Song, L. Meng, Z. He, J. Huang, F. Li, J. Feng, et al., LBP protects hepatocyte mitochondrial function via the PPAR-CYP4a2 signaling pathway in a rat sepsis model, Shock 56 (2021) 1066–1079.
[26] A.I. Legaki, I.I. Moustakas, M. Sikorska, G. Papadopoulos, R.I. Velliou, A. Chatzigeorgiou, Hepatocyte mitochondrial dynamics and bioenergetics in obesity-related non-alcoholic fatty liver disease, Curr. Obes. Rep. (2022), https://doi.org/10.1007/s13679-022-00473-1.
[27] I. Freitas, E. Boncompagni, E. Tarantola, C. Gruppi, V. Bertone, A. Ferrigno, et al., In situ evaluation of oxidative stress in rat fatty liver induced by a methionine-and choline-deficient diet, Oxid. Med Cell Longev. 2016 (2016), 9307064.
[28] H. Fang, A. Liu, O. Dirsch, U. Dahmen, Liver transplantation and inflammation: is lipopolysaccharide binding protein the link? Cytokine 64 (2013) 71–78.
[29] K.M. van der Heijden, I.M. van der Heijden, F.H. Galvao, C.G. Lopes, S.F. Costa, E. Abdala, et al., Intestinal translocation of clinical isolates of vancomycin-resistant Enterococcus faecalis and ESBL-producing Escherichia coli in a rat model of bacterial colonization and liver ischemia/reperfusion injury, PLOS One 9 (2014), e108453.
[30] G. Tsoulfas, Y. Takahashi, R.W. Ganster, G. Yagnik, Z. Guo, J.J. Fung, et al., Activation of the lipopolysaccharide signaling pathway in hepatic transplantation preservation injury, Transplantation 74 (2002) 7–13.
[31] M. Guerville, A. Leroy, A. Sinquin, F. Laugerette, M.C. Michalski, G. Boudry, Western-diet consumption induces alteration of barrier function mechanisms in the ileum that correlates with metabolic endotoxemia in rats, Am. J. Physiol. Endocrinol. Metab. 313 (2017) E107–E120.
[32] P.D. Cani, J. Amar, M.A. Iglesias, M. Poggi, C. Knauf, D. Bastelica, et al., Metabolic endotoxemia initiates obesity and insulin resistance, Diabetes 56 (2007) 1761–1772.